Tropospheric ozone distributions over Europe during the heat wave in July 2007 observed from infrared nadir spectra recorded by IASI

M. Eremenko, G. Dufour, Gilles Foret, C. Keim, J. Orphal, M. Beekmann, G. Bergametti, J.-M. Flaud

GEOPHYSICAL RESEARCH LETTERS, VOL. 35, L18805, doi:10.1029/2008GL034803, 2008

Tropospheric ozone distributions over Europe during the heat wave in July 2007 observed from infrared nadir spectra recorded by IASI

M. Eremenko,[1] G. Dufour,[1] G. Foret,[1] C. Keim,[1] J. Orphal,[1] M. Beekmann,[1] G. Bergametti,[1] and J.-M. Flaud[1]

Received 27 May 2008; revised 17 July 2008; accepted 5 August 2008; published 23 September 2008.

[1] First partial tropospheric ozone columns (0–6 km) derived from radiances observed by the IASI instrument aboard the MetOp-A platform over Europe during summer 2007 are presented. They were retrieved using an altitude-dependent regularization method. Comparison with measurements from balloon sondes shows excellent agreement. Space-borne observations show large lower tropospheric ozone amounts over South-Eastern Europe during the heat wave period, which are also displayed by simulations with a regional chemistry-transport model CHIMERE. **Citation:** Eremenko, M., G. Dufour, G. Foret, C. Keim, J. Orphal, M. Beekmann, G. Bergametti, and J.-M. Flaud (2008), Tropospheric ozone distributions over Europe during the heat wave in July 2007 observed from infrared nadir spectra recorded by IASI, *Geophys. Res. Lett.*, *35*, L18805, doi:10.1029/2008GL034803.

1. Introduction

[2] Ozone (O_3) is a key species for tropospheric chemistry affecting the troposphere's oxidative capacity, its radiative balance and air quality [*Finlayson-Pitts and Pitts*, 1999]. Its monitoring is essential to quantify its sources, transport, chemical transformation [*Clerbaux et al.*, 2004] and to evaluate global and regional models used for climate and pollution modeling. Synergistic use of models and observations (e.g., assimilation) is important to better assess the tropospheric O_3 budget and improve the predictions of chemical weather and climate. In addition to in situ measurements, satellite observations are very promising due to their large spatial coverage.

[3] Tropospheric O_3 retrieval from satellite observations is a challenging task because only a small part of the total atmospheric O_3 is contained in the troposphere. Up to now, satellite O_3 measurements are made mainly using ultraviolet-visible sounders [e.g., *Valks et al.*, 2003; *Liu et al.*, 2006; *Schoeberl et al.*, 2007]. However, the recent development of infrared nadir sounders allows detection of tropospheric ozone. In particular, tropospheric O_3 column measurements using infrared spectra has been first demonstrated using IMG (Interferometric Monitor for Greenhouse gases) [e.g., *Coheur et al.*, 2005] and more recently using TES (Tropospheric Emission Spectrometer) [e.g., *Worden et al.*, 2007] satellite data.

[4] Here, we present first results of tropospheric O_3 measured with the Infrared Atmospheric Sounding Interferometer (IASI) launched in October 2006 onboard the satellite MetOp-A. The used retrieval method allows separating the tropospheric O_3 columns into two semi-independent columns and demonstrates the potential of IASI to measure the lower tropospheric O_3 variability. The IASI observations used here focus on the heat wave in July 2007 over Europe. These observations are compared to O_3 balloon sonde measurements and to predictions from the CHIMERE model for validation and interpretation.

2. The IASI Instrument

[5] The IASI instrument [*Clerbaux et al.*, 2007] is an operational meteorological instrument. In addition to temperature and humidity profiles and cloud information, providing spatial distributions of O_3 is one of the objectives. IASI measures the thermal infrared radiation (TIR) emitted by the Earth's surface and the atmosphere. It is a Fourier transform spectrometer with a 2 cm optical path difference covering the 645–2760 cm^{-1} range. The apodized spectral resolution is 0.5 cm^{-1} (Full-Width at Half-Maximum). The radiometric accuracy in noise-equivalent radiance temperature at 280K is 0.28 K at 650 cm^{-1} and 0.47 K at 2400 cm^{-1}. Note that no operational Level 2 data (clouds, surface temperatures, temperature vertical profiles) necessary for O_3 retrieval are available for the summer 2007 period. Thus, all these parameters were retrieved from the IASI Level 1 data (spectra) as described in section 3.2. The MetOp-A satellite flies in a polar sun-synchronous orbit (about 800 km altitude) and comes over Europe about twice per day (at 9h30 and 21h30). The size of the IASI field-of-view is 12 km (at the sub-satellite point), and one swath of IASI covers about 2200 km in the West-East direction perpendicular to the satellite's orbit. Compared to IMG and TES it is important to highlight the much higher spectral coverage by IASI.

3. Methodology

3.1. Definition of the Constraint Matrix Using the Altitude Dependent Regularization

[6] The objective is to retrieve as precisely as possible the tropospheric O_3 distribution from IASI spectra with a maximum of information on the vertical distribution. Atmospheric inversions usually lead to ill-posed problems and need a constrained nonlinear least squares fitting solution as extensively detailed by *Rodgers* [2000, chapter 5]. The choice of the constraint is crucial in order to optimize the number of independent pieces of information on the vertical

[1]Laboratoire Interuniversitaire des Systèmes Atmosphériques, UMR7583, Université Paris-Est and Université Denis Diderot–Paris 7, CNRS, Créteil, France.

0094-8276/08/2008GL034803$05.00

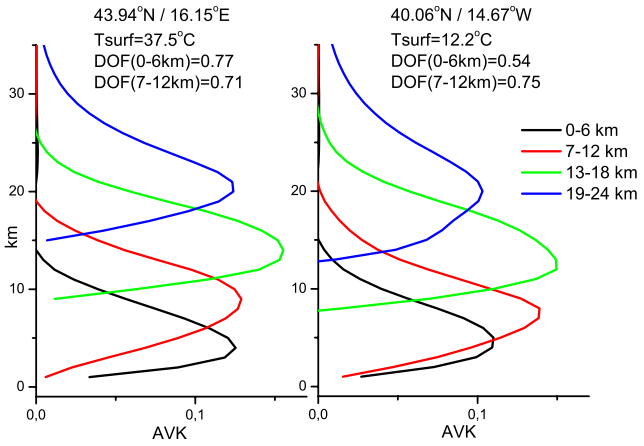

Figure 1. Comparison of averaging kernels in partial column space for conditions of (left) hot and (right) cold surface temperature.

concentration profile. Here, we choose to apply an analytical altitude-dependent regularization method rather than the widely used optimal estimation method. Actually, the former method is more flexible because the constraint and the number of pieces of independent information are not determined by the a-priori knowledge (climatology), and therefore permits to increase the freedom of the solution in adequacy with the maximum of sensitivity of the measurement (where the atmospheric variability is usually small resulting in strong constraint with the optimal estimation method). The method is therefore better adapted to the retrieval of unusual O_3 concentrations, for example during strong pollution events.

[7] Whereas the strength of the constraint in the classical regularization method [*Tikhonov*, 1963] is the same for all the altitudes, it may be dependent of the altitude for particular atmospheric retrieval methods [*Kulawik et al.*, 2006; *Doicu et al.*, 2004]. We applied a method similar to *Kulawik et al.* [2006] with the constraint matrix expressed as:

$$\mathbf{R} = \alpha_0(z)\mathbf{L}_0\mathbf{L}_0^T + \alpha_1(z)\mathbf{L}_1\mathbf{L}_1^T + \alpha_2(z)\mathbf{L}_2\mathbf{L}_2^T \quad (1)$$

[8] L_0, L_1 and L_2 are respectively the identity matrix, the first or the second derivative operator. The α_0, α_1 and α_2 coefficients are functions of altitude optimized using a simplex method. The optimization criterion is based on a compromise between the minimization of the retrieved profile error and the maximization of the freedom of the solution. According to *Kulawik et al.* [2006], the best figure of merit is $ERR/DOF^{1/8}$ where $ERR = \sqrt{trace(S_{tot})/n}$ is the mean error calculated for the total error S_{tot} over n tropospheric levels (equation (3)).

[9] Taking the formalism of *Rodgers* [2000], the retrieval is characterized by (i) the averaging kernel (AVK) **A** (equation (2)) that describes the sensitivity of the retrieval to the true state, (ii) the degrees of freedom (DOF) of the solution ($DOF = trace(\mathbf{A})$), and (iii) the error estimate (equation (3)).

$$\mathbf{A} = \left(\mathbf{K}_i^T\mathbf{S}_\varepsilon^{-1}\mathbf{K}_i + \mathbf{R}\right)^{-1}\mathbf{K}_i^T S_\varepsilon^{-1}\mathbf{K} \quad (2)$$

[10] **K** is the Jacobian of the forward model with respect to atmospheric state vector, S_ε is the measurement error covariance matrix, $\mathbf{x}_a$ is the a priori vector (which is also set as the first guess).

[11] In this formalism, the total error is obtained as the sum

$$\mathbf{S}_{tot} = \mathbf{S}_{meas} + \mathbf{S}_{temp} + \mathbf{S}_{smooth} + \mathbf{S}_{syst} \quad (3)$$

where $\mathbf{S}_{meas}$, $\mathbf{S}_{temp}$, $\mathbf{S}_{smooth}$ are the measurement noise error, the temperature profile error and the smoothing error respectively, calculated according to *Rodgers* [2000]. $\mathbf{S}_{syst}$ represents the other systematic error contributions estimated using a linear mapping of the parameter uncertainty on the resulting mixing ratio. The final product used in this paper is the partial tropospheric O_3 column calculated as the discrete sum of the O_3 concentration multiplied by the layer width.

[12] Its error is evaluated by:

$$\mathbf{S}_{column} = \sum_{i,j=1}^{N} S_{tot}(i,j)dens(i)dens(j)h(i)h(j) \quad (4)$$

[13] $\mathbf{S}_{tot}$ is the total error matrix, $dens(i)$ is the atmospheric density for the layer i and $h(i)$ is the thickness of the layer.

3.2. Characteristics of the Retrievals

[14] Auxiliary data are retrieved before the O_3 retrieval. The surface temperature is retrieved from selected microwindows between 800 and 950 cm^{-1} that are weakly sensitive to the absorption by atmospheric gases. The vertical temperature profile is retrieved from CO_2 lines (670–700 cm^{-1}). We applied a rather simple method with two steps to identify clear-sky scenes and to check the quality of the spectra: (i) rejection of unreasonably cold spectra (considering the season and the location, the threshold in surface temperature was fixed to 275 K) that allows filtering opaque clouds seen in TIR as cold surfaces; (ii) rejection of spectra with a baseline distortion (compared to a black or grey body) detected in transparent microwindows (at about 831 and 957 cm^{-1}) that may be explained by the presence of (partial or semitransparent) clouds in the field of view [see *Schlüssel et al.*, 2004, Figure 3]. This filter allows eliminating potentially contaminated spectra that would bias the O_3 retrievals.

[15] Seven spectral windows in the 975–1100cm^{-1} spectral region have been selected for O_3 retrieval in order to limit the influence of the H_2O uncertainties in the retrievals. The spectroscopic parameters are from the MIPAS database [*Flaud et al.*, 2003] for O_3 and HITRAN 2004 [*Rothman et al.*, 2005] for the other species. The KOPRA [*Stiller et al.*, 1998] radiative transfer code and its retrieval tool, both adapted to the nadir-viewing geometry and the altitude-dependent regularization, are used. Figure 1 shows typical averaging kernels of our retrievals for high and low surface temperatures. The retrieved O_3 profile (given in volume mixing ratio by altitude) may be separated into two semi-independent columns in the troposphere. The DOF for the 0–6 km column are 0.77 and 0.54 for these two typical cases of high and low European summer surface temperatures. The 1σ total estimated errors for these partial columns are

Table 1. Comparison of Satellite Derived O_3 Partial Columns Between 0 and 6 km With Coincident O_3 Sonde Measurements

Sonde Station	Latitude and Longitude	Number of Coincidences	Mean Column[a] (DU)	Bias (DU)	Bias (%)	R	RMS Differences (DU)	Total Column Error[b] (%)
Hohenpeissenberg	47.80, 11.02	10	20.1	0.4	1.8	0.91	1.7	14.8
Payerne	46.49, 6.57	16	19.3	0.1	0.8	0.96	1.1	16.1
Lindenberg	52.21, 14.12	14	26.4	−3.0	−11.6	0.85	3.8	16.0
Barajas/Madrid	40.47, −3.58	5	21.7	0.5	2.8	0.79	1.8	11.0
Total		45	21.9	−0.8	−2.6	0.87	2.4	10.2

[a]For satellite derived 0–6km columns. Note: the a priori column value is 26.4 DU for all cases.
[b]Estimated as explained in section 3.

10.5% and 19.7%. For comparison, the DOF are 1.48 and 1.29 for the 0–12 km column and the error is 5.0% and 7.1%, and for the total ozone column the DOF are 3.90 and 3.58 and the total error is 1.9% and 2.2%. The error is calculated using equation (4) with a noise-equivalent spectral radiance of 20 nW/(cm^{2}srcm^{-1}) for the noise contribution and a 2K uncertainty for the temperature profile contribution. Concerning the other systematic errors, only uncertainties in O_3 line positions (0.001 cm^{-1}) and intensities (1%) have a significant contribution. The smoothing part of the total error and the a priori are estimated using the climatology of *McPeters et al.* [2007] for mid-latitude summer conditions. It is worth noting that all the retrievals are then based on a single a priori (independent of the location).

4. Comparison With in Situ Measurements

[16] In order to evaluate the quality of the retrieved O_3 columns, they were compared to World Ozone and Ultraviolet Data Center (WOUDC) balloon sonde data http://www.woudc.org/). At the time of the study, measurements for only 4 sites were available over Europe between June and August 2007. For each O_3 sonde profile, only cloud-free IASI measurements coincident within one degree with respect to the station coordinates and measured the same morning were considered. For a total of 45 chosen sonde measurements, we compared the averaged IASI columns matching the coincidence criteria (between 4 and 12 cloud-free IASI pixels per sonde) with the sonde profiles smoothed by the IASI averaging kernels [*Worden et al.*, 2007, equation (5)]. The results of comparison are summarized in Table 1. Figure 2 shows the time series of the 0–6 km partial O_3 columns measured by IASI and sondes at the 4 stations. The agreement between IASI and sonde measurements is very good with a mean bias smaller than 5% (except one site) and large temporal correlations (≥ 0.85, except one site with only 4 measurements). For all sites, differences remain within the error limits of the retrieval. This preliminary validation exercise shows that our retrieval method is rather consistent and relevant to retrieve tropospheric O_3 from IASI.

5. Comparison With Simulated Lower Tropospheric Ozone Columns

[17] In order to further interpret spatial consistency of our retrieved tropospheric O_3 columns and also to evaluate the potential gain to use IASI observations as an objective constraint for pollution models, first comparisons with the

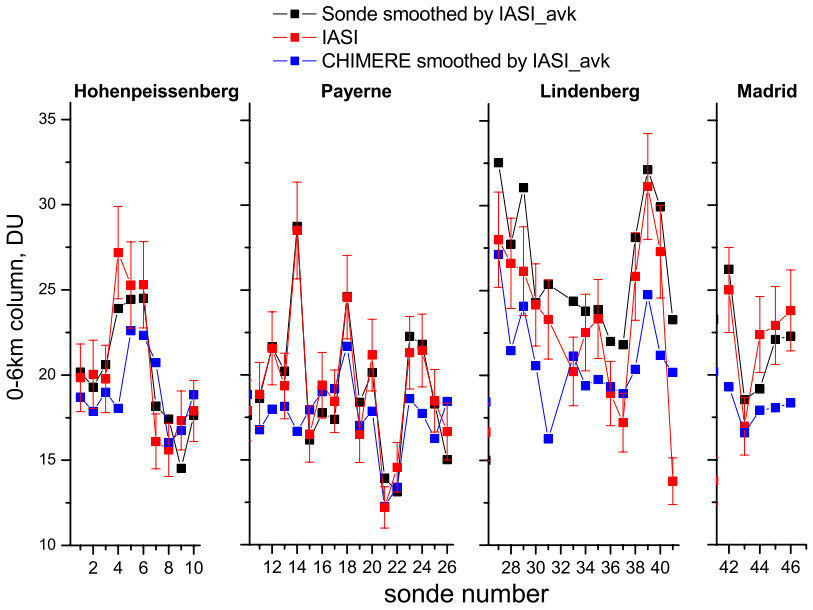

Figure 2. Partial (0–6 km) O_3 columns for coincident O_3 sonde and IASI measurements, and for CHIMERE simulations.

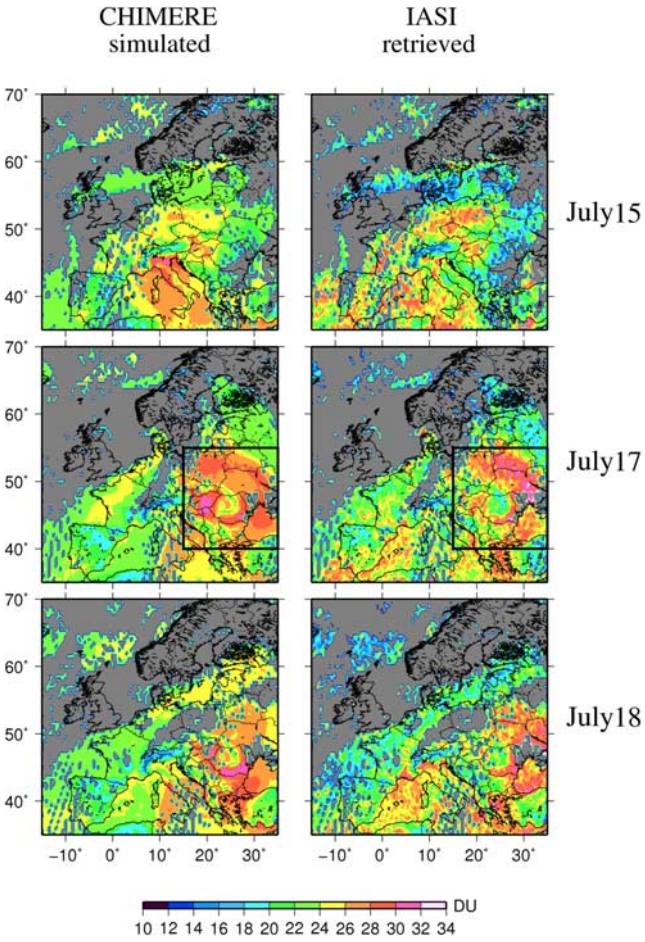

Figure 3. (left) Lower tropospheric O_3 columns predicted by CHIMERE (0–6 km) compared to (right) IASI retrieved lower tropospheric O_3 columns (0–6 km) for the morning passes of the satellite for (top) 15 July 2007, (middle) 17 July 2007 and (bottom) 18 July 2007. The observations have been interpolated on the 0.5 × 0.5 degrees grid of the model for comparison. Cloudy pixels are represented in grey.

regional chemistry and transport model CHIMERE [*Schmidt et al.*, 2001] have been performed. We used the continental version of CHIMERE http://euler.lmd.polytechnique.fr/chimere) vertically extended to the entire troposphere [*Blond et al.*, 2007]. The model runs with a horizontal resolution of 0.5° × 0.5° and with 17 vertical layers from the surface up to 200 hPa. It is driven by the European Center for Medium-Range Weather Forecasts meteorological analyses. LMDz-INCA monthly mean concentrations are used as boundary conditions [*Hauglustaine et al.*, 2004]. The CHIMERE model has been extensively evaluated against surface O_3 measurements over Europe showing very good agreement for daily O_3 maxima (e.g., averaged bias below 10%, correlation about 80%) [*Honoré et al.*, 2008].

[18] First, simulated 0–6 km O_3 columns (smoothed by the averaging kernels of IASI) at each sonde station are plotted in Figure 2 for comparison. Modeled O_3 columns show a reasonable agreement with the sonde and satellite measurements, the temporal variability of observed O_3 concentrations is with few exceptions well caught by the model. On average, modeled O_3 concentrations are lower than observed ones, especially at Lindenberg and Madrid. It is not possible in the framework of this study to firmly identify reasons of such discrepancies, but it can be speculated that they are related to the use of a monthly climatology at the lateral and top model boundaries and discrepancies in vertical transport, both affecting in particular free tropospheric O_3 levels.

[19] We then compare IASI O_3 partial columns retrieved for clear-sky scenes to simulated ones over Europe (Figure 3). We have chosen 3 days (15, 17 and 18 of July 2007) during the heat wave period over Eastern Europe (14–21 July 2007) during which persistent anticyclonic conditions [*European Environment Agency*, 2008] favored the occurrence of high O_3 concentrations. Especially, both observations and simulations show high O_3 column fields moving clockwise from Central to Eastern Europe with a singular structure over Romania. A statistical analysis (Figure 4) over this particular region (marked out by a square in Figure 3) shows a mean bias between observed and simulated columns of about - 4%. The root-mean-square (RMS) differences between the observations and the simulations are about 11% and comparable to uncertainties in measured columns. The spatial correlation (0.64) in the selected region is clearly significant (Figure 4). It is also noted that modeled O_3 fields exhibit lower variability than observed ones, simulations ranging from 21 to 32 DU with respect to 16–34 DU for observations. Outside of the selected region, larger differences are apparent, up to 20%, especially over the South-Western Mediterranean Sea. It is striking that larger (smaller) differences are related to regions with lower (higher) boundary layer (BL) height. For instance, in the heat wave region, exceptionally elevated BL heights are simulated (3 km and more already in the morning hours) and more than 50 % of O_3 of the 0–6 km partial columns is located within the BL. Indeed, CHIMERE is expected to better simulate boundary layer O_3 formed by photochemical processes than free tropospheric O_3 which is to a larger extend governed by boundary conditions.

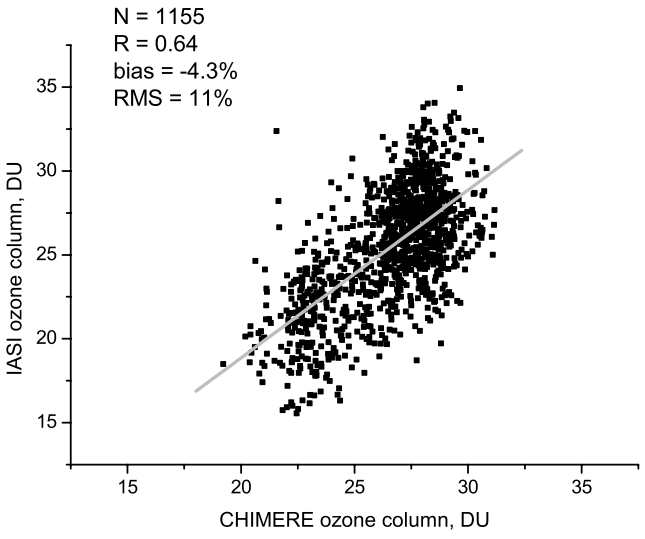

Figure 4. Correlation of the tropospheric O_3 columns observed by IASI and predicted by the CHIMERE model for the O_3 polluted area indicated on Figure 3.

[20] As a conclusion, our results show that skillful lower tropospheric O_3 columns can be derived from IASI. The agreement with O_3 sonde measurements is excellent and comparisons with regional air quality model (CHIMERE) simulations show that the main structures of tropospheric O_3 fields are well captured by the observations. This work states the capabilities of the new generation of nadir infrared sounders to provide information on tropospheric O_3 relevant for air quality studies and also to give an objective constraint to the air quality models especially in the free troposphere where model evaluation has been difficult due to the lack of in situ measurements with enough spatial coverage.

[21] **Acknowledgments.** We wish to thank the Institut für Meteorologie und Klimaforschung (IMK), Karlsruhe, Germany, for a licence to use the KOPRA radiative transfer model, and the ETHER database (CNRS, INSU, CNES) in France for providing access to IASI Level 1 data. We acknowledge the World Ozone and Ultraviolet Data Center (WOUDC) for making the routine ozone sonde measurements accessible. This study was supported by the French Space Agency CNES (project "IASI-TOSCA"). C.K. thanks the French Space Agency CNES for a post-doctoral fellowship.

References

Blond, N., K. F. Boersma, H. J. Eskes, R. J. van der A, M. Van Roozendael, I. De Smedt, G. Bergametti, and R. Vautard (2007), Intercomparison of SCIAMACHY nitrogen dioxide observations, in situ measurements and air quality modeling results over Western Europe, *J. Geophys. Res.*, *112*, D10311, doi:10.1029/2006JD007277.

Clerbaux, C., J. Gille, and D. Edwards (2004), New directions: Infrared measurements of atmospheric pollution from space, *Atmos. Environ.*, *38*, 4599–4601.

Clerbaux, C., et al. (2007), The IASI/MetOp I mission: First observations and highlights of its potential contribution to GMES, *Space Res. Today*, *168*, 19–24.

Coheur, P.-F., B. Barret, S. Turquety, D. Hurtmans, J. Hadji-Lazaro, and C. Clerbaux (2005), Retrieval and characterization of ozone vertical profiles from a thermal infrared nadir sounder, *J. Geophys. Res.*, *110*, D24303, doi:10.1029/2005JD005845.

European Environment Agency (2008), Air pollution by ozone across Europe during summer 2007, *EEA Tech. Rep. N5/2008*, Eur. Environ. Agency, Copenhagen.

Doicu, A., F. Schreier, and M. Hess (2004), Iterative regularization methods for atmospheric remote sensing, *J. Quant. Spectrosc. Radiat. Transfer*, *83*, 47–61.

Finlayson-Pitts, B. J., and J. N. Pitts (1999), *Chemistry of the Upper and Lower Atmosphere: Theory, Experiments, and Applications*, 969 pp., Academic, San Diego, Calif.

Flaud, J.-M., C. Piccolo, B. Carli, A. Perrin, L. H. Coudert, J.-L. Teffo, and L. R. Brown (2003), Molecular line parameters for the MIPAS (Michelson Interferometer for Passive Atmospheric Sounding) experiment, *Atmos. Oceanic Opt.*, *16*, 172–182.

Hauglustaine, D. A., F. Hourdin, L. Jourdain, M.-A. Filiberti, S. Walters, J.-F. Lamarque, and E. A. Holland (2004), Interactive chemistry in the Laboratoire de Météorologie Dynamique general circulation model: Description and background tropospheric chemistry evaluation, *J. Geophys. Res.*, *109*, D04314, doi:10.1029/2003JD003957.

Honoré, C., et al. (2008), Predictability of European air quality: Assessment of 3 years of operational forecasts and analyses by the PREV'AIR system, *J. Geophys. Res.*, *113*, D04301, doi:10.1029/2007JD008761.

Kulawik, S. S., G. Osterman, D. B. A. Jones, and K. W. Bowman (2006), Calculation of altitude-dependent Tikhonov constraints for TES nadir retrievals, *IEEE Trans. Geosci. Remote Sens.*, *44*, 1334–1342, doi:10.1109/TGRS.2006.871206.

Liu, X., et al. (2006), First directly retrieved global distribution of tropospheric column ozone from GOME: Comparison with the GEOS-CHEM model, *J. Geophys. Res.*, *111*, D02308, doi:10.1029/2005JD006564.

McPeters, R. D., G. J. Labow, and J. A. Logan (2007), Ozone climatological profiles for satellite retrieval algorithms, *J. Geophys. Res.*, *112*, D05308, doi:10.1029/2005JD006823.

Rodgers, C. D. (2000), *Inverse Methods for Atmospheric Sounding: Theory and Practice*, 200 pp., World Sci., Hackensack, N. J.

Rothman, L. S., et al. (2005), The HITRAN 2004 molecular spectroscopic database, *J. Quant. Spectrosc. Radiat. Transfer*, *96*, 139–204.

Schoeberl, M. R., et al. (2007), A trajectory-based estimate of the tropospheric ozone column using the residual method, *J. Geophys. Res.*, *112*, D24S49, doi:10.1029/2007JD008773.

Schlüssel, P., T. H. Hultberg, P. L. Phillips, T. August, and X. Calbet (2004), The operational IASI level 2 processor, *Adv. Space Res.*, *36*(5), 982–988.

Schmidt, H., C. Derognat, R. Vautard, and M. Beekmann (2001), A comparison of simulated and observed ozone mixing ratios for summer of 1998 in western Europe, *Atmos. Environ.*, *35*, 6277–6297.

Stiller, G. P., et al. (1998), The Karlsruhe optimized and precise radiative transfer algorithm. Part I: Requirements, justification, and model error estimation, in *Optical Remote Sensing of the Atmosphere and Clouds*, edited by J. Wang et al., *Proc. SPIE, 3501*, 257–268.

Tikhonov, A. (1963), On the solution of incorrectly stated problems and a method of regularization, *Dokl. Acad. Nauk SSSR*, *151*, 501–504.

Valks, P. J. M., R. B. A. Koelemeijer, M. van Weele, P. van Velthoven, J. P. F. Fortuin, and H. Kelder (2003), Variability in tropical tropospheric ozone: Analysis with Global Ozone Monitoring Experiment observations and a global model, *J. Geophys. Res.*, *108*(D11), 4328, doi:10.1029/2002JD002894.

Worden, H. M., et al. (2007), Comparisons of Tropospheric Emission Spectrometer (TES) ozone profiles to ozonesondes: Methods and initial results, *J. Geophys. Res.*, *112*, D03309, doi:10.1029/2006JD007258.

M. Beekmann, G. Bergametti, G. Dufour, M. Eremenko, J.-M. Flaud, G. Foret, C. Keim, and J. Orphal, Laboratoire Interuniversitaire des Systèmes Atmosphériques, UMR7583, Université Paris-Est, CNRS, F-94010 Créteil, France. (eremenko@lisa.univ-paris12.fr)